Criterion for the Design of Low-Power Variable Stiffness Mechanisms

Vincent Chalvet and David J. Braun

***Abstract*—Designing robotic systems capable of low-power operation, inherent to their compliant actuation, has been elusive in practical application. In this paper, we propose a physical measure to mathematically define mechanical designs that are suitable to realize stiffness modulation with low power cost. Using this measure, we present a mathematical formulation of an ideal variable stiffness mechanism unaffected by the external load during its operation. We then analyze several existing mechanisms from the literature to relate design features with analytical conditions inherent to low power stiffness modulation in practical designs. Through this analysis, we identify an approximate practical realization of an ideal actuator capable of stiffness modulation with inherently low power cost. Similar to a number of existing efficient variable stiffness mechanisms, this mechanism is able to hold a given stiffness setting with zero input force under no external load. However, unlike many other previously designed mechanisms, it enables infinite range stiffness modulation using finite control forces. A practical variable stiffness mechanism that is capable of infinite range stiffness modulation using finite control forces leads to lower power cost and reduced energy consumption.**

***Index Terms*—Analytical design conditions, variable stiffness mechanisms.**

I. Introduction

Compliant actuators [1], used in variety of robotic applications, provide several advantages over traditional stiff joints, including lower reflected inertia [2], better shock absorption [2], safer human–robot interaction [3], capacity for energy storage [4], as well as adaptability of the mechanical embodiment to the control task [5], [6]. The ability to control not only the output force but also the stiffness of variable stiffness actuators [7]–[12] makes them suitable to develop new generation robots, as well as biologically compatible assistive technology, i.e., prosthetic, orthotics, and wearable exoskeleton devices [13], [14]. In particular, the possibility to achieve inherently stable open-loop stiffness modulation—independently of the stiffness setting—could set these actuators apart from noncompliant and nonvariable stiffness actuators. However, the extent of stiffness modulation, typically achieved on variable stiffness actuators, is limited in range and is energetically expensive, hindering the promise of the variable stiffness actuation technology for decades. There has been a number of recent efforts addressing these issues by utilizing sophisticated control approaches [6], developing mathematical design frameworks [15], as well as realizing intrinsically energy efficient actuators [12], [16], [17]. Nevertheless, the design of actuators enabling inherently low power stiffness modulation remains difficult in practical application.

Actuators are often characterized by their efficiency. Efficiency quantifies the power transferred from the motor at the actuator's input to the load at the actuator's output. It is commonly perceived that higher efficiency makes the actuator better suited to robotic applications, i.e., higher energy efficiency means that larger part of the work done by the motor at the input is transferred to the load at the actuator's output. However, on variable stiffness systems, the work done by the motor at the actuator's input is not always converted to work at the actuator's output. In turn, the motor unit may require power in adjusting and maintaining the apparent stiffness of the actuator when the output link remains at a fixed configuration. The mechanical work generated at the actuator's output is zero in that case, and as such the usual efficiency measure does not provide a meaningful characterization of the energetic benefit of the actuator. It is the stiffness adjusting subsystem that requires input energy for stiffness modulation while it may not do any work at the output of the actuator.

There has been a number of previous efforts, aiming to characterize the energetic consequence of stiffness modulation, by using the input mechanical power of the stiffness modulating motor. Unlike the usual efficiency measure, the input mechanical power provides a better characterization of the energy required for stiffness modulation on variable stiffness actuators [15], [17]–[19]. However, the mechanical power by the motor can be zero even when electrical power is drained for stiffness holding. This is to say that, just like the usual efficiency measure, the mechanical power may not provide complete information required to characterize the suitability of the actuator design to perform low power stiffness modulation. Providing a physical measure, which can be used to quantify the inherent energetic benefits of topologically different variable stiffness designs is vital to analitically define, objectively cross-compare, computationally design, and mathematically classify novel design solutions.

In this paper, we present a physical measure that quantifies the energetic consequence of different variable stiffness mechanical designs. To do this, we analyze the power required by the driving motor due to the internal forces born during stiffness modulation in variable stiffness actuators. Through this analysis, we identify the magnitude of the input force—force imposed by the stiffness modulating mechanism to the motor unit—to provide a measurable and physically interpretable metric that characterizes the power drained for stiffness modulation irrespective of the particular use (motion) of the actuator. By setting this input force to zero, we define an ideal actuator which is unaffected by the external load during stiffness modulation (i.e., a mechanism that requires zero energy to hold a stiffness setting during its operation). Subsequently, we compare six existing variable stiffness mechanisms in terms of their stiffness range and suitability to provide stiffness modulation with inherently low power cost. Through this comparison, we identify three analytical conditions to certify mechanisms capability of low power stiffness modulation, and show that a simple variable length leaf-spring mechanism may be used as an approximate practical realization of the ideal actuator dedicated to stiffness modulation. Similar to other intrinsically efficient variable stiffness mechanisms, this

Manuscript received May 12, 2016; revised October 21, 2016; accepted February 24, 2017. Date of publication May 16, 2017; date of current version August 7, 2017. This paper was recommended for publication by Associate Editor S. Kim and Editor I.-M. Chen upon evaluation of the reviewers' comments. This work was supported by the SUTD-MIT International Design Center as part of the Energy-Efficient Compliant Actuator Designs Project (IDG31400108). *(Corresponding author: David J. Braun.)*

The authors are with the Dynamics and Control Laboratory within the Engineering Product Development Pillar, Singapore University of Technology and Design, Singapore 487372, Singapore (e-mail: vincent_chalvet@sutd.edu.sg; david_braun@sutd.edu.sg).

Color versions of one or more of the figures in this paper are available online at http://ieeexplore.ieee.org.

Digital Object Identifier 10.1109/TRO.2017.2689068

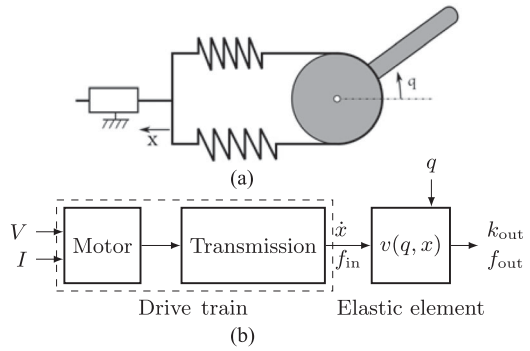

Fig. 1. Model of a variable stiffness mechanism. (a) Example of an antagonistic variable stiffness mechanism. (b) Schematic representation of the stiffness modulating subsystem, where V denotes the applied voltage to the motor, I denotes the motor current, $\dot{x}$ is the velocity at the input to the mechanism, f_{in} is the force imposed by the mechanism to the drive-train, f_{out} is the output force, while k_{out} is the output stiffness of the actuator.

leaf-spring mechanism is able to hold a given stiffness setting with zero input force under no external load, but unlike many other previously designed mechanisms, it enables infinite range stiffness modulation using finite control forces. This result leads to a new class of variable stiffness mechanisms.

II. Variable Stiffness Mechanisms

Variable stiffness actuators are actuators that employ two motors at their input to provide concurrent modulation of the elastic force and stiffness at their output. A unique part of these actuators is a stiffness modulating mechanism that employs at least one motor at its input to provide variable stiffness at its output. An example of such mechanism is shown in Fig. 1(a). By changing the motor position, the apparent output stiffness of the joint can be directly modulated.

The complete representation of the stiffness modulating subsystem [depicted in Fig. 1(b)] is provided by the model of the drive-train and the potential energy function of the stiffness modulating mechanism. The potential energy function is defined by

$$v(q,x) = \sum_{i=1}^{N} \int_{l_{i0}}^{l_i(q,x)} f_i(l)dl \tag{1}$$

where f_i denotes the forces by the N elastic elements (of length l_i and equilibrium length l_{i0}) embedded in the design, $q \in \mathbb{R}$ defines the output position, and $x \in \mathbb{R}$ defines the input position.

Using this potential energy function, the input force (felt by the motor) the output force (generated by the mechanism) and the apparent output stiffness are defined by

$$f_{\text{in}}(q,x) = \frac{\partial v}{\partial x}, \quad f_{\text{out}}(q,x) = -\frac{\partial v}{\partial q} \quad \text{and} \quad k_{\text{out}}(q,x) = \frac{\partial^2 v}{\partial q^2}. \tag{2}$$

The model of the drive-train, motor, and transmission [see Fig. 1(b)], is given by the following two equations:

$$\begin{aligned} \text{FT:} \quad & (\eta_{\text{f}} n^2 m_{\text{m}} + m_{\text{t}})\ddot{x} + (\eta_{\text{f}} n^2 \gamma_{\text{eq}} + \gamma_{\text{t}})\dot{x} = n\eta_{\text{f}} f_{\text{m}} - f_{\text{in}} \\ \text{BT:} \quad & (n^2 m_{\text{m}} + \eta_{\text{b}} m_{\text{t}})\ddot{x} + (n^2 \gamma_{\text{eq}} + \eta_{\text{b}} \gamma_{\text{t}})\dot{x} = n f_{\text{m}} - \eta_{\text{b}} f_{\text{in}} \end{aligned} \tag{3}$$

where m_{m} is the inertia of the motor, m_{t} is the inertia of the transmission line, n is the transmission ratio, $\gamma_{\text{eq}} = \gamma_{\text{m}} + k_{\text{m}}^2 R_{\text{m}}^{-1}$ is the damping of the motor [this includes the mechanical damping and the damping due to the back electromotive force], γ_{t} is the damping of the transmission line, $f_{\text{m}} = k_{\text{m}} R_{\text{m}}^{-1} V$ is the force generated by the motor, k_{m} is the motor torque constant, R_{m} is the electrical winding resistance, V is the input voltage, and η_{f} and η_{b} denote the efficiency of the drive-train in forward transmission (FT) when power is transmitted from the motor to the variable stiffness mechanism, and in backward transmission (BT) when power is transmitted from the variable stiffness mechanism to the motor.[1]

The input force f_{in}, last term in the right-hand side of (3), appears due to the coupling between the drive-train and the variable stiffness mechanism. It is this force—to be opposed or overcome by the motor—that can be significant even when stiffness is not modulated, i.e., when $\dot{x} = 0 \Rightarrow f_{\text{m}} \propto f_{\text{in}}$. This feature is present, regardless of how the mechanism is controlled, and this is one of the features that hindered low-power variable stiffness actuation for decades. In the following, we will investigate this issue by focusing on kinematic features of variable stiffness mechanisms, and the energetic consequence of stiffness modulation on topologically different mechanical designs.

A. Ideal Variable Stiffness Mechanism

In this paper, we use the total electrical power of the stiffness modulating motor unit to characterize the energy cost of stiffness modulation on variable stiffness systems. This motor power, expressed in the mechanical domain, is given by the following relation:

$$p(x,\dot{x},\ddot{x},f_{\text{in}}) = IV = p_0(x,\dot{x},\ddot{x}) + f_{\text{in}}(w_1\ddot{x} + w_2\dot{x}) + w_3 f_{\text{in}}^2 \tag{4}$$

where w_1, w_2, and w_3 are positive constants that depend on the physical parameters of the drive-train and the direction of the power flow.[2] The first term in the above relation $p_0(x,\dot{x},\ddot{x})$ is the power drained by the motor assuming that the stiffness modulating mechanism does not impose any force on the motor. On the other hand, the last two terms represent the added power due to the reaction force implied by stiffness modulation. More specifically, the last two terms are associated with two different modes of operation, i.e., while $f_{\text{in}}(w_1\ddot{x} + w_2\dot{x})$ is only present during stiffness tuning, $w_3 f_{\text{in}}^2$ indicates the power required to hold a given stiffness setting.

According to the above relation (4), minimizing the three coefficients w_1, w_2, and w_3 is one way to minimize the power drained by the motor performing stiffness modulation. In particular, this can be done by using a nonbackdrivable drive-train ($\eta_{\text{b}} = 0$ implying $w_1 = w_2 = w_3 = 0$ in backward drive), which can completely eliminate the effect of the stiffness modulating mechanism on the motor unit. However, nonbackdrivable drive-trains lead to inherently inefficient designs when used in forward drive (low η_{f}), and as such, utilizing this solution to cancel the power required for stiffness modulation, or to hold the stiffness of the actuator, does not generally provide an advantageous variable stiffness design. In turn, it is the drive-train and not the stiffness adjusting mechanism that is used to eliminate the last component in (4) while making the cost of stiffness modulation high in such designs.

Based on the above argument, and by using (4), we define an ideal variable stiffness mechanism as the one that does not impose any force on the drive-train (and the motor unit) irrespective of the way stiffness is modulated. This means that, while stiffness can be modulated, the

[1]The transmission efficiency depends on the type of the actuator. In particular, for an ideal back-drivable actuator the backward efficiency is the same as the forward efficiency $\eta_{\text{b}} = \eta_{\text{f}}$ while for nonbackdrivable actuators the backward efficiency is zero.

[2]Expression (4) is calculated using: $V = f_{\text{m}} R_{\text{m}} k_{\text{m}}^{-1}$, $I = R_{\text{m}}^{-1}(V - k_{\text{m}} n\dot{x})$ and (3). The parameters in this expression are defined by: $w_1 = 2R_{\text{m}}/(k_{\text{m}}n)^2(m_{\text{m}}n^2 + m_{\text{t}}\eta)\eta$, $w_2 = 2R_{\text{m}}/(k_{\text{m}}n)^2(\gamma_{\text{m}}n^2 + \gamma_{\text{t}}\eta)\eta + \eta$ and $w_3 = R_{\text{m}}\eta^2/(k_{\text{m}}n)^2$, where we denote $\eta = \eta_{\text{f}}^{-1}$ in the case of forward transmission (FT) and $\eta = \eta_{\text{b}}$ during backward transmission (BT) respectively.

input force must be zero on the ideal mechanism:

$$\frac{\partial k_{\text{out}}(q,x)}{\partial x} \neq 0 \quad \text{and} \quad f_{\text{in}}(q,x) = 0. \tag{5}$$

This definition implies zero input mechanical power $f_{\text{in}}\dot{x} = 0$. However, the condition that asserts zero mechanical power does not define the ideal mechanism. This is because the mechanical power could be zero when $\dot{x} = 0$ while the input force may not be zero, i.e., power may be used according to the last term in (4). While designing a real actuator that satisfies the second condition in (5) may not be feasible, the insight gained by the above definition suggests a physical measure that can be used to characterize designs suitable for low power stiffness modulation.

B. Criterion for the Design of Low-Power Variable Stiffness Mechanisms

Following the definition of the ideal variable stiffness design, we propose the squared input force to be a metric which defines "how far" a given mechanical design is from the ideal design for stiffness modulation[3]:

$$\mathrm{d}(f_{\text{in}}, 0) = f_{\text{in}}^2. \tag{6}$$

According to this definition, the ideal design is given by $\mathrm{d}(f_{\text{in}}, 0) = 0$. In relation to the power consumed by the actuator, this design metric turns out to be proportional to the static motor power required to hold a given stiffness setting in backdrivable actuators, i.e., $\ddot{x} = \dot{x} = 0 \Rightarrow p \propto f_{\text{in}}^2$. We note that the proposed design metric and the total electrical power (4) are not directly proportional in general. However, reducing this metric by changing the mechanical design will also reduce the total power during stiffness modulation. This assertion turns out to be true, irrespective of whether holding or changing stiffness is considered, and irrespective of whether the transmission line is back-drivable or nonbackdrivable by design.[4] This is what justifies the introduction of the above metric to characterize mechanical designs suitable to inherently low power stiffness modulation.

Our design metric differs from results of related previous works in two important ways. First, unlike the metric derived using mechanical domain models of variable stiffness actuators [19], our metric captures the energetic consequence of stiffness modulation even in the case when the mechanical power of the motor is zero i.e., no mechanical work is done by the actuator. To ensure this, it is essential to take into account the electrical-side dynamics when considering the energetics of variable stiffness actuators. Second, unlike analytical conditions [15], our metric is measurable and as such can be used to experimentally quantify the suitability of practical designs in realizing low energy stiffness modulation (Section V). In the following, we will use the proposed metric (6) to first classify six variable stiffness mechanisms from the literature (Section III) and then define a new class of mechanisms capable of infinite range stiffness modulation using low power cost (Section IV).

[3]This metric defines the difference between a real and the ideal actuator. In case of redundant actuation, realized with multiple motors, this design metric is defined by: $\mathrm{d}(\mathbf{f}_{\text{in}}, \mathbf{0}) = \mathbf{f}_{\text{in}}^{\mathrm{T}}\mathbf{f}_{\text{in}}$.

[4]For a nonbackdrivable drive-train design, the power drained by the motor is zero when the mechanism is used to hold a given stiffness setting, but it is nonzero, and depends on the input force (4), when the mechanism changes the actuator's stiffness setting. This is why the proposed design metric can be used to characterize actuators that require inherently low power for stiffness modulation even if their drive-train is nonbackdrivable by design.

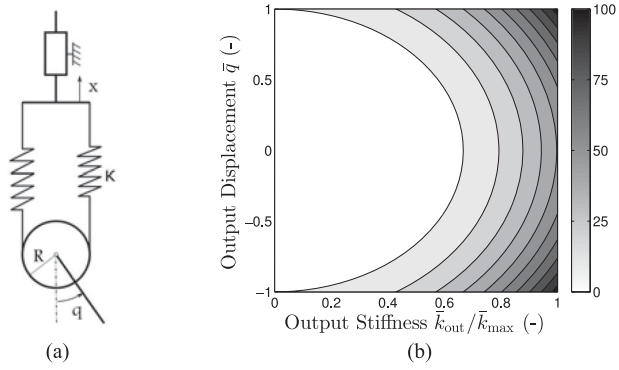

(a) (b)

Fig. 2. Antagonistic variable stiffness mechanism. (a) Schematic representation of the reduced mechanism dedicated to stiffness modulation. (b) Squared input force $\bar{f}_{\text{in}}^2$ over the workspace of the mechanism. The black lines denote constant $\bar{f}_{\text{in}}^2$ curves. Darker colors denote higher values of the force.

III. Comparison of Variable Stiffness Designs

Modulating the output stiffness on series elastic or variable stiffness actuators typically leads to high energy cost. On series elastic actuators, the closed-loop control augmenting the actuator's passive structure is what leads to high energy cost. On variable stiffness actuators, the additional motor unit and the stiffness modulating subsystem are the components that lead to added and often high energy cost. In this Section we analyze the stiffness modulating subsystem of the following actuators:

1) biologically inspired antagonistic actuator [10];
2) mechanically adjustable compliance and controllable equilibrium position actuator (MACCEPA) [20];
3) variable stiffness joint (VS-Joint) [11];
4) actuator with adjustable stiffness (AwAS) [17];
5) variable stiffness actuator with variable lever arm (VSAwVLA) [19]; and the
6) variable length leaf-spring mechanism (VLLSM) [21].

The purpose of this analysis is to identify the analytical conditions characterizing actuators capable of stiffness modulation with inherently low power cost.

A. Antagonistic Variable Stiffness Mechanism

Antagonistic variable stiffness actuators [9], [10], [22], [23] make use of two motor units and two springs in order to modulate the output force and the output stiffness of the joint. The output force of these actuators depends on the difference between the motor positions, whereas the output stiffness depends on the sum of the motor positions. Figure 2(a) shows an antagonistic mechanism that employs a single motor to perform stiffness modulation. The potential energy of this mechanism is given by $v(q,x) = \frac{1}{3}\kappa\left[(x+qR)^3 + (x-qR)^3\right]$ where κ is the pseudo-stiffness of the springs,[5] while R is the radius of the pulley. By introducing the dimensionless input position $\bar{x} = x/R$, output position $\bar{q} = q$ and the dimensionless potential energy function $\bar{v}(\bar{q},\bar{x}) = v/(2\kappa R^3) = \frac{1}{3}\bar{x}(3\bar{q}^2 + \bar{x}^2)$, we derive the dimensionless output stiffness and the dimensionless input force for this mechanism

$$\bar{k}_{\text{out}}(\bar{x}) = \partial^2\bar{v}/\partial\bar{q}^2 = 2\bar{x} \quad \text{and} \quad \bar{f}_{\text{in}}(\bar{q},\bar{x}) = \partial\bar{v}/\partial\bar{x} = \bar{q}^2 + \bar{x}^2 \tag{7}$$

where $(\bar{q},\bar{x}) \in \mathcal{S} = \{\mathbb{R}^2 : 0 \leq \bar{x} \leq \bar{x}_{\max}, 0 \leq \bar{x} \pm \bar{q} \leq \bar{\delta}\}$ is the feasible workspace. These constraints ensure that the springs are always

[5]As opposed to typical linear springs, the springs in this mechanism have quadratic force-deflection characteristic.

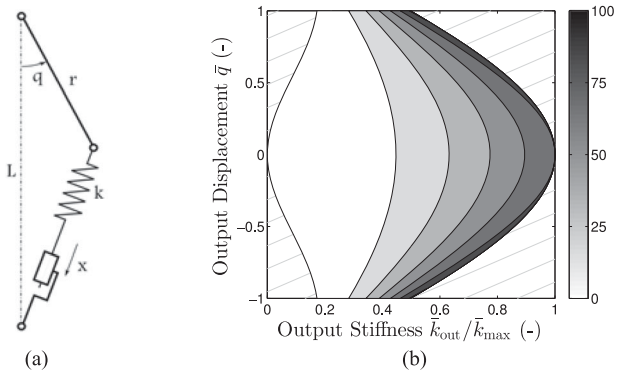

Fig. 3. MACCEPA—(a) Schematic representation of the stiffness adjusting subsystem. (b) Squared input force $\bar{f}_{\text{in}}^2$ over the workspace of the mechanism. The dimensionless model parameter is $\bar{r} = 1/5$. The plot represents a typical behavior of this system.

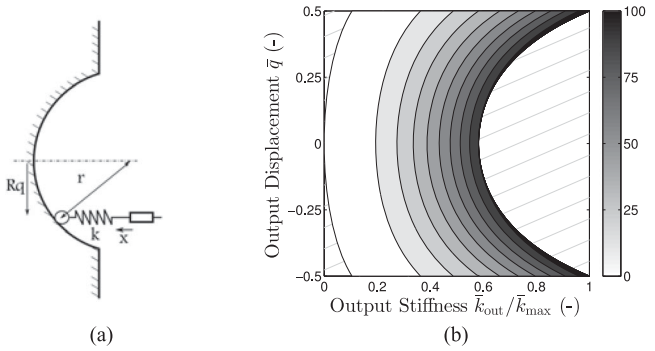

Fig. 4. VS-Joint—(a) Schematic representation of the stiffness modulating mechanism. (b) Squared input force $\bar{f}_{\text{in}}^2$ over the workspace of the mechanism.

extended, and that they do not exceed their maximum allowable deformation $\bar{\delta} > 0$.

The size of this mechanism is defined by the motion range of the stiffness adjusting motor, i.e., $\bar{x} \in [0, \bar{x}_{\max}]$. For this reason, and according to the first relation in (7), the stiffness range of this mechanism is limited, i.e., $0 \leq \bar{k}_{\text{out}}(\bar{x}) \leq 2\bar{x}_{\max}$.

In Fig. 2(b), we show the distribution of the squared input force as a function of the output displacement and the output stiffness of the mechanism. We observe that when the mechanism is at its equilibrium configuration ($\bar{q} = 0$), the input force depends on the square of the output stiffness

$$\bar{f}_{\text{in}}(\bar{q}, \bar{x}) = \bar{k}_{\text{out}}(\bar{x})^2/4 + \bar{q}^2 \tag{8}$$

thereby indicating that increasing the stiffness leads to high input force even if the mechanism is not displaced from its equilibrium configuration. The input force will furthermore increase when external load is applied at the output, i.e., when the mechanism is displaced from its equilibrium configuration ($\bar{q} \neq 0$). As a result, the input force in this mechanism may only be low for small values of the apparent output stiffness.

B. Mechanically Adjustable Compliant Actuator

Figure 3(a) shows the stiffness adjusting mechanism used in the MACCEPA introduced in [20]. Similar to the antagonistic actuator considered in Section III-A, the stiffness of this mechanism can be modulated by adjusting the pretension of the spring. However, unlike in the antagonistic mechanism, there is only one spring in this design, and this spring is linear. Stiffness modulation is achieved through nonlinear geometric coupling between the actuator's position input and its output.

The dimensionless potential energy of this mechanism is given by $\bar{v}(\bar{q}, \bar{x}) = v/(kL^2) = \frac{1}{2}[\bar{x} + \bar{r} - 1 + \bar{\Delta}(\bar{q})^{\frac{1}{2}}]^2$ where $\bar{\Delta}(\bar{q}) = 1 + \bar{r}^2 - 2\bar{r}\cos\bar{q}$ represents a geometric quantity, $\bar{x} = x/L$ is the dimensionless input position, $\bar{q} = q$ is the dimensionless output position, $\bar{r} = r/L \in (0, 1)$ is a geometric parameter, while the physical parameters (length of the crank r, size of the mechanism L, and the stiffness of the spring k) are shown in Fig. 3(a). Using $\bar{v}(\bar{q}, \bar{x})$, the dimensionless output stiffness and the dimensionless input force are given by

$$\bar{k}_{\text{out}}(\bar{q}, \bar{x}) = \bar{r}\cos\bar{q} - \frac{(\bar{r} + \bar{x} - 1)}{\bar{\Delta}(\bar{q})^{3/2}}\bar{r}[\bar{r}(1 + \cos^2\bar{q}) - \cos\bar{q}(1 + \bar{r}^2)],$$

$$\bar{f}_{\text{in}}(\bar{q}, \bar{x}) = \bar{x} + \bar{r} - 1 + \bar{\Delta}(\bar{q})^{\frac{1}{2}} \tag{9}$$

where $(\bar{q}, \bar{x}) \in \mathcal{S} = \{\mathbb{R}^2 : 0 \leq \bar{x} \leq \bar{x}_{\max}, 0 \leq \bar{r} + \bar{x} + \bar{\Delta}(\bar{q})^{\frac{1}{2}} - 1 \leq \bar{\delta}\}$ defines the feasible workspace. Like in the antagonistic mechanism, the stiffness range in this system is limited by the motion range of the motor. This is shown by the following relation $0 \leq \bar{k}_{\text{out}}(0, \bar{x}) \leq \bar{r}/(1 - \bar{r})\bar{x}_{\max}$.

Figure 3(b) shows the squared input force as a function of the output position $\bar{q}$ and the output stiffness $\bar{k}_{\text{out}}$. Similar to the antagonistic actuator, considered in Section III-A, here the input force also depends on the output stiffness $\bar{k}_{\text{out}}$ even if the mechanism is not displaced from its equilibrium configuration

$$\bar{f}_{\text{in}}(\bar{q}, \bar{x})|_{\bar{q} \approx 0} \approx (1 - \bar{r})\bar{k}_{\text{out}}(0, \bar{x})/\bar{r} + \bar{r}\bar{q}^2/(2 - 2\bar{r}). \tag{10}$$

This means that higher stiffness leads to higher input force and as such potentially higher power drained during the operation of this actuator. In addition, the input force will increase when the output position is deflected from its equilibrium configuration, i.e., when $\bar{q} \neq 0$ [see Fig. 3(b)].

C. Variable Stiffness Joint

Figure 4(a) shows the stiffness modulating mechanism used in the VS-Joint introduced in [11]. In this design, the displacement of the output link q leads to the motion of a circular roller which, in turn, compresses the spring inbuilt in the mechanism. Stiffness adjustment is realized by changing the internal geometry of the device x, i.e., compressing the springs with a motor.

The dimensionless potential energy of this mechanism is given by $\bar{v}(\bar{q}, \bar{x}) = v/(kr^2) = \frac{1}{2}[1 + \bar{x} - (1 - \bar{q}^2)^{\frac{1}{2}}]^2$ where $\bar{x} = x/r$ is the input position, $\bar{q} = (R/r)q$ is the output position, while the physical parameters (radius of the circular cam r, moment arm of the output link R, and the stiffness of the spring k) are shown in Fig. 4(a). Using this potential energy function, the output stiffness and the input force of this mechanism are given by the following dimensionless relations:

$$\bar{k}_{\text{out}}(\bar{q}, \bar{x}) = \frac{(1 + \bar{x})}{(1 - \bar{q}^2)^{\frac{3}{2}}} - 1, \quad \bar{f}_{\text{in}}(\bar{q}, \bar{x}) = 1 + \bar{x} - (1 - \bar{q}^2)^{\frac{1}{2}}. \tag{11}$$

The feasible workspace of this mechanism is defined by $(\bar{q}, \bar{x}) \in \mathcal{S} = \{\mathbb{R}^2 : 0 \leq \bar{x} \leq \bar{x}_{\max}, 0 \leq 1 + \bar{x} - (1 - \bar{q}^2)^{\frac{1}{2}} \leq \bar{\delta}\}$. Just like in the previous two cases, the stiffness range is limited on this mechanism. This may be best seen by considering the stiffness at the equilibrium configuration $0 \leq \bar{k}_{\text{out}}(0, \bar{x}) \leq \bar{x}_{\max}$.

Figure 4(b) shows the squared input force as a function of the output position and output stiffness of this mechanism. Similar to the previous mechanism, the input force depends linearly on the output stiffness and

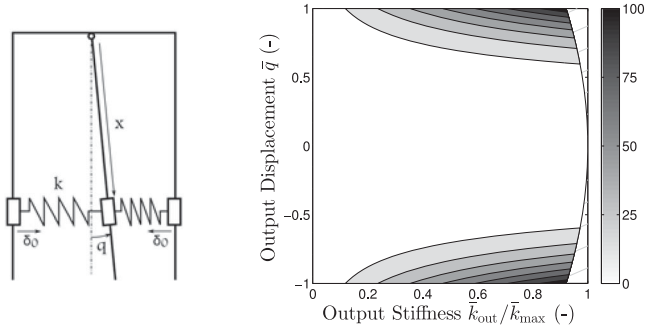

(a) (b)

Fig. 5. AwAS—(a) Schematic representation of the stiffness adjusting mechanism. (b) Squared input force $\bar{f}_{\text{in}}^2$ over the workspace of this stiffness tuning mechanism.

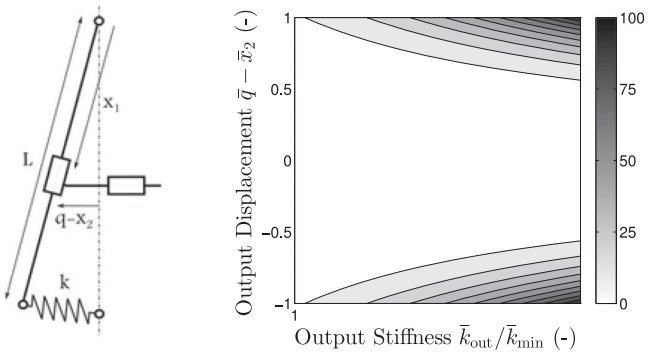

(a) (b)

Fig. 6. VSAwVLA—(a) Schematic representation. (b) Squared input force $\bar{f}_{\text{in}}^2$ over the workspace of this stiffness tuning mechanism.

quadratically on the output position around the equilibrium configuration

$$\bar{f}_{\text{in}}(\bar{q},\bar{x})|_{\bar{q}\approx 0} \approx \bar{k}_{\text{out}}(0,\bar{x}) + \bar{q}^2/2. \tag{12}$$

The previous three mechanisms are characterized by a monotonically increasing relation between the stiffness and the proposed design metric. In Section IV-A, we show that this general feature defines a class of variable stiffness mechanisms. Spring pretension-based mechanisms belong to this class.

D. Actuator With Adjustable Stiffness

Figure 5(a) shows a schematic representation of the AwAS introduced in [17]. This mechanism makes use of two precompressed springs positioned on both sides of the output link. By moving the slider along the link, the apparent stiffness of the rotational joint can be modulated.

The dimensionless potential energy of this mechanism is given by $\bar{v}(\bar{q},\bar{x}) = v/(2k\delta_0^2) = \frac{1}{2}\left[1+\bar{x}^2\sin^2\bar{q}\right]$ where $\bar{x} = x/\delta_0$ and $\bar{q} = q$ are the dimensionless input and output positions, while the physical parameters (stiffness k and the precompression δ_0 of the springs) are shown in Fig. 5(a). Using this potential energy function, the dimensionless output stiffness and the input force are given by

$$\bar{k}_{\text{out}}(\bar{q},\bar{x}) = \bar{x}^2\cos(2\bar{q}), \quad \bar{f}_{\text{in}}(\bar{q},\bar{x}) = \bar{x}\sin^2(\bar{q}). \tag{13}$$

The workspace of this mechanism is given by $(\bar{q},\bar{x}) \in \mathcal{S} = \{\mathbb{R}^2 : 0 \le \bar{x} \le \bar{x}_{\max}, 0 \le 1 \pm \bar{x}\sin(\bar{q}) \le \bar{\delta}\}$. According to (13), and similar to the previous three mechanisms, the output stiffness is limited by the size of this actuator. This feature can be seen by considering the stiffness at the equilibrium configuration $0 \le \bar{k}_{\text{out}}(0,\bar{x}) \le \bar{x}_{\max}^2$.

Figure 5(b) shows the squared input force as a function of the output position and the output stiffness of this mechanism. We note that the force distribution here differs from the force distribution seen in the previous examples. Most importantly, when the mechanism is not deflected from its equilibrium configuration, the input force is zero irrespective of the output stiffness. On the other hand, when external load is applied to this mechanism (when the output link is displaced from its equilibrium configuration $\bar{q} \neq 0$), the input force is proportional to the square root of the output stiffness and the square of the output displacement

$$\bar{f}_{\text{in}}(\bar{q},\bar{x})|_{\bar{q}\approx 0} \approx \bar{k}_{\text{out}}(0,\bar{x})^{\frac{1}{2}}\,\bar{q}^2. \tag{14}$$

This means that the input force can be kept low near to the equilibrium configuration regardless of the output stiffness of this mechanism.

E. Variable Stiffness Actuator With Variable Lever Arm

Figure 6(a) shows a variable stiffness design (VSAwVLA) introduced in [15]. The stiffness of this actuator can be directly modulated using a single motor $\bar{x}_1$. However, the actuator employs two motors, and by using the second motor $\bar{x}_2$, stiffness modulation can be realized in number of different ways. In particular, one may employ the second motor to implement stiffness modulation without changing the potential energy of the actuator. This way to perform stiffness modulation, under fixed output position, was previously proposed to achieve energy efficient variable stiffness actuation.[6]

The dimensionless potential energy of this mechanism is given by $\bar{v}(\bar{q},\bar{x}_1,\bar{x}_2) = v/(kL^2) = \frac{1}{2}[(\bar{q}-\bar{x}_2)/\bar{x}_1]^2$ where $\bar{x}_1 = x_1/L$ and $\bar{x}_2 = x_2/L$ denote the dimensionless input positions, $\bar{q} = q/L$ is the dimensionless output position, while the physical parameters (length of the lever-arm L and the spring stiffness k) are shown in Fig. 5(a). Using the dimensionless potential energy function, the dimensionless output stiffness and input forces are given by the following relations:

$$\bar{k}_{\text{out}} = 1/\bar{x}_1^2, \quad \bar{f}_{\text{in}1} = -(\bar{q}-\bar{x}_2)^2/\bar{x}_1^3, \quad \bar{f}_{\text{in}2} = (\bar{x}_2-\bar{q})/\bar{x}_1^2 \tag{15}$$

where $(\bar{q},\bar{x}_1,\bar{x}_2) \in \mathcal{S} = \{\mathbb{R}^3 : 0 \le \bar{x}_1 \le \bar{x}_{1\max}, 0 \le \bar{x}_2 \le \bar{x}_{2\max}, |\bar{q}-\bar{x}_2| \le \bar{\delta}\bar{x}_1\}$ defines the feasible workspace of the actuator, while $\bar{\delta}$ denotes the largest deflection of the spring.

Figure 6(b) shows the squared input force of the main motor $\bar{x}_1$ dedicated to stiffness modulation.[7] According to the output stiffness defined in (15), this design enables infinite range stiffness modulation $\bar{x}_{1\max}^{-2} \le \bar{k}_{\text{out}}(\bar{x}_1) \le \infty$. This is unlike all other previously analyzed mechanisms. Furthermore, we observe that similar to the AwAS mechanism presented in Section III-D, this actuator requires no input force when operated at its equilibrium configuration ($\bar{q} = \bar{x}_2$):

$$\bar{f}_{\text{in}1}(\bar{q},\bar{x}_1,\bar{x}_2) = -\bar{k}_{\text{out}}(\bar{x}_1)^{\frac{3}{2}}(\bar{q}-\bar{x}_2)^2. \tag{16}$$

The previous two mechanisms are characterized by zero input force when operated at their equilibrium configuration. In Section IV-A, we use this general feature to define a distinct class of variable stiffness mechanisms. Variable moment arm mechanisms belong to this class.

[6][15]: Energy efficient variable stiffness actuation can be obtained by changing the output stiffness without injecting or extracting energy to and from the elastic elements.

[7]The contribution of the second motor $\bar{x}_2$ is not shown in this plot. This is because the second motor would only increase the squared input force but could not change qualitatively the relation seen in Fig. 6(b).

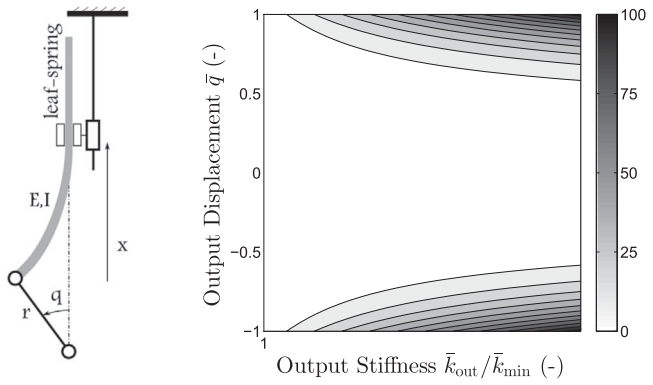

Fig. 7. VLLSM — (a) Schematic representation. (b) Squared input force $\bar{f}_{\rm in}^2$ over the workspace of this mechanism.

F. Variable Length Leaf-Spring Mechanism

Figure 7(a) shows the variable stiffness design (VLLSM) introduced in [21]. In this design, the elastic element—leaf-spring—is connected at one end to the output link while it is free at the other end. The output stiffness of this system is adjusted by changing the effective length of the leaf-spring using a position controlled slider.

The potential energy of this mechanism is given by $\bar{v}(\bar{q},\bar{x}) = \frac{2r}{3EI}v = \sin^2\bar{q}/\bar{x}^3$ where $\bar{x} = x/r$ is the dimensionless input position, $\bar{q} = q$ is the dimensionless output position, while the physical parameters (Young's modulus E, second moment of area I of the leaf-spring, and the length of the crank r) are shown in Fig. 7(a). Using this potential energy function, the dimensionless output stiffness and the input force are given by

$$\bar{k}_{\rm out}(\bar{q},\bar{x}) = 2\cos(2\bar{q})/\bar{x}^3, \;\; \bar{f}_{\rm in}(\bar{q},\bar{x}) = -3\sin^2\bar{q}/\bar{x}^4 \qquad (17)$$

where $(\bar{q},\bar{x}) \in \mathcal{S} = \{\mathbb{R}^2 : 0 \le \bar{x} \le \bar{x}_{\max}, |\sin(\bar{q})| \le \min[1, \bar{\delta}\bar{\sigma}_{\rm Y}\bar{x}^2]\}$ denotes the feasible workspace of this mechanism. These constraints ensure that the stress in the leaf-spring does not exceed the yield stress $\bar{\sigma}_{\rm Y}$, while $\bar{\delta}$ is the dimensionless geometric parameter of this actuator. According to the first expression above, the VLLSM can afford infinite-range stiffness modulation (irrespective of the limited size of the actuator) $2\bar{x}_{\max}^{-3} \le \bar{k}_{\rm out}(\bar{q},\bar{x}) \le \infty$.

Figure 7(b) shows the distribution of the squared input force over the workspace of this mechanism which is similar to the force distribution shown for the previous two mechanisms. Furthermore, according to the second expression above, this design does not require input force to hold a given stiffness setting when the output link is at the equilibrium configuration

$$\bar{f}_{\rm in}(\bar{q},\bar{x})|_{\bar{q}\approx 0} \approx -\frac{3}{2^{\frac{4}{3}}}\bar{k}_{\rm out}(0,\bar{x})^{\frac{4}{3}}\bar{q}^2. \qquad (18)$$

IV. Stiffness Modulation With Low Power Cost

According to the above analysis, the proposed design metric can be used to cross-compare mechanisms with different kinematic topology. In order to do this in a systematic and physically interpretable way, let us first decompose the design metric in the following way

$$\mathrm{d}(f_{\rm in},0) = \underbrace{\mathrm{d}(f_{\rm in}(0,x),0)}_{f_{\rm in}(0,x)^2} + \underbrace{\mathrm{d}(f_{\rm in}(q,x),0) - \mathrm{d}(f_{\rm in}(0,x),0)}_{f_{\rm in}(q,x)^2 - f_{\rm in}(0,x)^2}. \qquad (19)$$

The first component contains the squared input force required to hold a given stiffness setting under no external load, while the second component characterizes the added force when the actuator is under external load. Using this decomposition, we proceed with analytical classification of the previously considered mechanical designs. The purpose of this classification is to identify the ability of these actuators to perform low power cost stiffness modulation regardless of whether they are operated at or away from their equilibrium configuration.

A. Power Drain at the Equilibrium Configuration

The relation between the input force and the output stiffness at the equilibrium configuration (i.e., $q = 0$) has been derived in Section III for six different actuators. According to these relations, the squared input force at the equilibrium configuration is a monotonically increasing function of the output stiffness on the first three actuators (8), (10), (12). On the other hand, the AwAS, VSAwVLA, and the VLLSM do not require any force to hold a given stiffness setting, see (14), (16), and (18). This is to say that these three actuators behave like the ideal actuator (5) when operated at their equilibrium configuration

$$\mathrm{d}(f_{\rm in}(0,x),0) = f_{\rm in}(0,x)^2 = 0. \qquad (20)$$

In turn, the qualitative difference in the input force between the first three and the last three mechanisms, shown in Figs. 2(b)–7(b), is due to the force required to hold a desired stiffness at the equilibrium configuration. Our design metric makes a clear distinction between these two classes of mechanisms, indicating that mechanisms belonging to the first class—those that use spring pretension to change stiffness—are not capable of inherently low power stiffness modulation whereas mechanisms belonging to the second class—those that use some form of lever arm modulation—are capable of inherently low power stiffness modulation. While a similar conclusion has been known from the literature, our condition provides a physically interpretable mathematical characterization of designs capable of low power stiffness modulation.

B. Power Drain Away From the Equilibrium Configuration

As opposed to the previous consideration, the input force required to hold a given stiffness setting when the output position is displaced from the equilibrium configuration shows similar behavior for all six mechanisms analyzed in Section III. This behavior—exemplified by the quadratic dependence of the input force and the output displacement near to the equilibrium configuration—can be directly seen for the last three actuators, i.e., (14), (16), and (18).[8] According to (8), (10), and (12), the input force of the first three actuators is also quadratic with respect to q near to the equilibrium configuration.

Despite these similarities, there are some important differences between the latter three actuators. In turn, as indicated in Sections III-D and III-E, the stiffness range of the AwAS [17] is limited by the size of this actuator, while this is not the case on the VSAwVLA [15], which is capable of infinite range stiffness modulation. However, while the VSAwVLA allows infinite-range stiffness modulation, the input force, and as such the power drained by the motor dedicated to stiffness modulation, may tend to infinity as the stiffness approaches infinity on this actuator, i.e.,

$$\mathrm{d}(\bar{f}_{\rm in1}(\bar{q},\bar{x}),0) \le \max_{(\bar{q},\bar{x})\in\mathcal{S}} \bar{f}_{\rm in1}(\bar{q},\bar{x})^2 = \lim_{\bar{k}_{\rm out}\to\infty}[\bar{\delta}^4\bar{k}_{\rm out}] = \infty \qquad (21)$$

where $\mathcal{S}$ is the feasible workspace, while $\bar{\delta}$ is the largest spring deflection of this actuator (see Section III-E). According to this relation, infinite stiffness may not be attainable even if the input and output positions remain within the feasible workspace of this actuator. Contrary to this, the variable length leaf-spring mechanism (see

[8] This is because $\mathrm{d}(f_{\rm in}(0,x),0) = 0$ on these actuators.

Section III-F) is characterized by bounded input force over its workspace

$$\mathrm{d}(\bar{f}_{\text{in}}(\bar{q},\bar{x}),0) \leq \max_{(\bar{q},\bar{x})\in\mathcal{S}} \bar{f}_{\text{in}}(\bar{q},\bar{x})^2 \leq 9\left(\bar{\delta}\bar{\sigma}_{\text{Y}}\right)^4 < \infty \qquad (22)$$

where $\bar{\sigma}_{\text{Y}}$ denotes the dimensionless yield stress of the leaf-spring material. This is to say that, on the VLLSM, the input force remains bounded even if the mechanism is commanded to perform infinite-range stiffness modulation.

The above condition may generalize to some previously designed variable stiffness leaf-spring mechanism although the use of leaf-springs, as opposed to helical extension or compression springs, does not guarantee condition (22), and designs where the leaf-spring is pre-stressed may even violate condition (20). This is to say that the use of leaf-springs does not warrant intrinsically low power variable stiffness design.

C. Inherently Low Power Stiffness Modulation

The analysis presented in this paper leads to a new class of mechanical designs enabling wide range stiffness modulation with low power cost. The analytical characterization of this class of mechanisms is given by the following three conditions:

$$\text{C.1:}\quad \mathrm{d}(f_{\text{in}}(0,x),0) = 0,$$

$$\text{C.2:}\quad \max_{(q,x)\in\mathcal{S}\subset\mathbb{R}^2} k_{\text{out}} = \infty,$$

$$\text{C.3:}\quad \max_{(q,x)\in\mathcal{S}\subset\mathbb{R}^2} \mathrm{d}(f_{\text{in}}(q,x),0) < \infty.$$

The first condition C.1 ensures that the mechanism does not require input force to hold a given stiffness setting at the equilibrium configuration. The second condition C.2 ensures that the mechanism enables infinite range stiffness modulation. The third condition C.3 states that the input force imposed by the mechanism on the motor remains finite. We note that the second condition necessitates infinite stiffness range. While this can be ensured for any finite value of the mechanism's minimum stiffness, realizing low minimum stiffness may also be desirable in practical application. This is indeed possible on some of the actuators satisfying the first condition above, such as the AwAS, but this actuator does not allow infinite-range stiffness modulation. On the other hand, the VLLSM satisfies all three conditions above, but it does not allow zero stiffness operation (at its equilibrium configuration). Despite this, due to the highly nonlinear relation between the output stiffness and the input position [see (17)], the minimum achievable stiffness can be made rather low on this design even for a relatively compact actuator.

Finally, we note that pretension-based variable stiffness mechanisms do not satisfy condition C.1 and as such they are not well suited to low power stiffness modulation. On the other hand, there are different variable moment arm mechanisms that do satisfy the first condition C.1 and have been previously classified as intrinsically efficient actuators. In this paper, we define a subclass of these mechanisms that enable infinite range stiffness modulation C.2 with finite input forces C.3. We envision these conditions to be useful when characterizing and designing new types of variable stiffness actuators, capable of more efficient and low power stiffness modulation.

V. Classification of Variable Stiffness Mechanisms

In this section, we show how to use the proposed metric to experimentally classify existing mechanisms without relying on details of their particular design. In order to demonstrate this, we consider the VLLSM [21] shown in Fig. 8. The model of this mechanism is presented in Section III-F. Using this model, we show that this mechanism

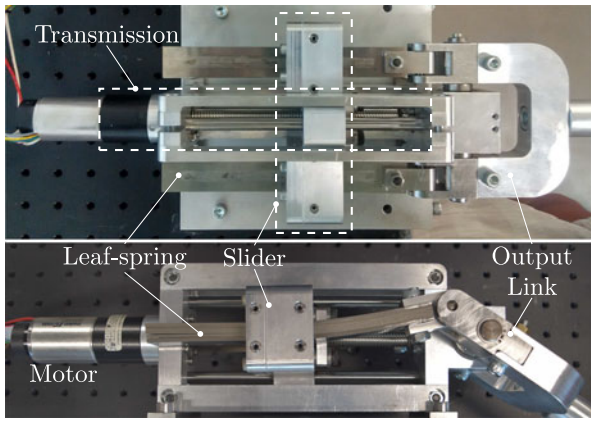

Fig. 8. VLLSM [21]—The device changes stiffness by changing the effective length of a leaf-spring. Two stacks of leaf-springs are used as elastic elements ($w \times [h]$: $20 \times [5 \times 1 + 10 \times 0.5]$ mm each, made from stainless steel of yield strength $\sigma_{\text{Y}} = 1250$ MPa). On one side, the spring is connected to the output shaft via a cylindrical joint while on the other side the spring is free. The effective length of the leaf-springs is modulated by a position controlled slider. The slider is moved using a *backdrivable* drive-train (using a 40 W 24 V brushless DC motor, 4.8:1 planetary gearbox, and a 2-mm pitch ball-screw). The motor is controlled using a Maxon ESCON 50/5 driver.

fulfills all three design conditions (C.1–C.3) presented in Section IV, and as such, it represents an intrinsically low-power design capable of large range stiffness modulation. We present experimental evidence supporting the three main assertions of the above analysis by which:

1) the actuator drains a small amount—theoretically zero—power at its equilibrium configuration (C.1);
2) the actuator is capable of reaching large—theoretically infinite—stiffness (C.2); and
3) irrespective of the stiffness of the actuator, the motor force and as such the power drained by the motor remains bounded during its operation (C.3).

The measurements of the current required by the motor to hold a given stiffness setting were performed in the following way: The motor was set to a desired position $x \in [0, 90]$ mm; the output link was then displaced from its equilibrium position $q \in [0, \pi/4]$. Once the dynamic behavior settled, the current, drained by the motor controller was measured. Using this current, the input force is computed. As a result, the distribution of the static motor force over the feasible workspace of the actuator is obtained.

Figure 9 shows the results of these measurements—static motor power as a function of the output stiffness k_{out} and the output position q of the actuator. The baseline motor power $p_{s0} \approx 1.44$ W corresponds to the power required by the controller (Maxon ESCON 50/5) alone. The difference between this baseline power and the largest power drained by the motor $p_{\text{smax}} \approx 2.16$ W defines the upper bound of the power required to hold a given stiffness on this actuator. According to the experimental results:

1) The input force is largely independent of the output stiffness at the equilibrium of this mechanism (see Fig. 9 $q \approx 0 \Rightarrow f_{\text{in}}^2 \approx 0$). This provides an experimental confirmation of the first condition (C.1) characterizing mechanical designs capable of low power stiffness modulation.
2) The mechanism has large stiffness range $\max[k_{\text{out}}] \approx 2.5 \times 10^5$ N·m/rad. In the largest stiffness configuration, we experimentally confirmed that the joint can only be slightly moved away from its equilibrium configuration (see Fig. 9 $k_{\text{out}} \to \infty \Rightarrow q \approx 0$), providing high stiffness under practical conditions.

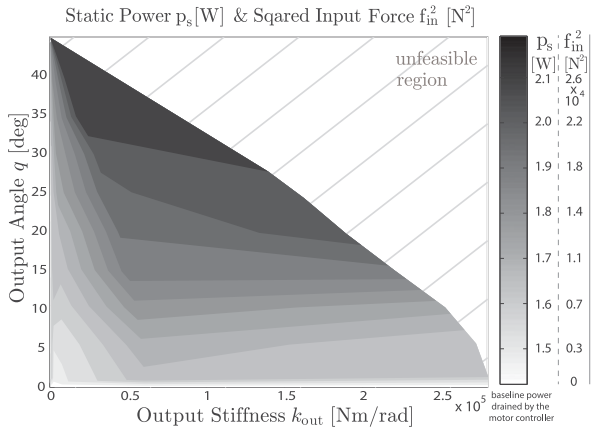

Fig. 9. Static motor power p_s and the squared input force $f_{\text{in}}^2 = (p_s - p_{s0})/w_3$ as functions of the output stiffness and the output position of the VLLSM. The lowest power drained by the motor controller alone corresponds to zero input force. The highest power corresponds to $f_{\text{in}} \approx 200$ N input force. The power drained by the motor controller alone would lead to two times higher input force on this actuator. The hatched area indicates unfeasible configurations. This area is present due to stress constraints, limiting the stiffness and motion range of this actuator, and the relation between the output position and the output stiffness, preventing high stiffness and high displacement to be simultaneously reached on this actuator. This area is not in the feasible set $\mathcal{S}$ defined in Section III-F.

3) The input force is finite regardless of the stiffness setting. In particular, we observe decreased input force (and power drain) at high stiffness (light gray in Fig. 9).

Figure 9 resembles[9] the analytical relation (17) between the squared input force, the output position, and the output stiffness. This result supports the qualitative predictions drawn from the minimalistic model used in Section III-F. Figure 9 also shows the relation between the static motor power and the squared input force which can be used to experimentally identify the design metric defined in this paper.

The above analysis demonstrates the practical realizability of a new class of variable stiffness mechanisms introduced in this paper. This analysis, however, does not address the question of how to design similar mechanisms that can reduce the power required for stiffness modulation due to their design. One way to do this is to combine a clutch-type drive-train with a series elastic actuator, not necessarily designed for low power stiffness modulation. This could eliminate the power required for stiffness holding and could enable discrete ON–OFF type stiffness modulation [24]. Alternatively, it may also be possible to design the stiffness modulating mechanism to avoid the forces generated by the elastic element to be directly transferred through the driving motor. This can be achieved by designing the geometry of the mechanism in such a way that the elastic element does not generate force which needs to be supported by the driving motor. However, none of these intuitive design recommendations warrant infinite range stiffness modulation using finite control forces. This is why, as an alternative to these considerations, one may adapt the proposed metric to computationally find mechanisms that enable low power stiffness modulation. This may be achieved by minimizing the proposed metric (6) to find near-ideal mechanisms that drain little power for stiffness modulation irrespective of their operation.

[9]The unfeasible region seen in Fig. 9 (hatched) is not shown in Figs. 2(b)–7(b). The qualitative similarity between Figs. 9 and 7(b) can be recognized by observing the shape of the isolines in these plots.

VI. Conclusion

In this paper, we presented a physical measure to quantify the energetic implications of different variable stiffness designs. Using this measure, we analyzed six existing mechanisms to identify mathematical conditions that warrant low-power cost stiffness modulating designs. Based on this analysis, we identified three analytical conditions, leading to a new class of variable stiffness mechanisms, enabling stiffness modulation with intrinsically low power cost. Our design conditions ensure zero control force when the actuator is operated at its equilibrium configuration, and infinite range stiffness modulation with finite control forces. We showed experimental results supporting these features on a prototype variable stiffness design.

References

[1] R. Van Ham, T. G. Sugar, B. Vanderborght, K. W. Hollander, and D. Lefeber, "Compliant actuator designs," *IEEE Robot. Autom. Mag.*, vol. 16, no. 3, pp. 81–94, Sep. 2009.
[2] G. A. Pratt and M. M. Williamson, "Series elastic actuators," in *Proc. IEEE/RSJ Int. Conf. Intel. Robot. Syst.*, 1995, pp. 399–406.
[3] A. Bicchi and G. Tonietti, "Fast and "soft-arm" tactics," *IEEE Robot. Autom. Mag.*, vol. 11, no. 2, pp. 22–33, Jun. 2004.
[4] J. W. Hurst, J. E. Chestnutt, and A. A. Rizzi, "The actuator with mechanically adjustable series compliance," *IEEE Trans. Robot.*, vol. 26, no. 4, pp. 597–606, Aug. 2010.
[5] D. J. Braun, M. Howard, and S. Vijayakumar, "Exploiting variable stiffness in explosive movement tasks," in *Proc. Robot., Sci. Syst.*, 2011, pp. 25–32.
[6] D. J. Braun *et al.*,"Robots driven by compliant actuators: Optimal control under actuation constraints," *IEEE Trans. Robot.*, vol. 29, no. 5, pp. 1085–1101, Oct. 2013.
[7] K. F. Laurin-Kovitz, J. E. Colgate, and S. D. Carnes, "Design of components for programmable passive impedance," in *Proc. IEEE Int. Conf. Robot. Autom.*, 1991, pp. 1476–1481.
[8] T. Morita and S. Sugano, "Design and development of a new robot joint using a mechanical impedance adjuster," in *Proc. IEEE Int. Conf. Robot. Autom.*, 1995, vol. 3, pp. 2469–2475.
[9] C. English and D. Russell, "Implementation of variable joint stiffness through antagonistic actuation using rolamite springs," *Mech. Mach. Theory*, vol. 34, no. 1, pp. 27–40, 1999.
[10] S. A. Migliore, E. A. Brown, and S. P. DeWeerth, "Novel nonlinear elastic actuators for passively controlling robotic joint compliance," *J. Mech. Des.*, vol. 129, no. 4, pp. 406–412, 2007.
[11] S. Wolf and G. Hirzinger, "A new variable stiffness design: Matching requirements of the next robot generation," in *Proc. IEEE Int. Conf. Robot. Autom.*, 2008, pp. 1741–1746.
[12] J. Choi, S. Hong, W. Lee, S. Kang, and M. Kim, "A robot joint with variable stiffness using leaf springs," *IEEE Trans. Robot.*, vol. 27, no. 2, pp. 229–238, Apr. 2011.
[13] A. M. Dollar and H. Herr, "Lower extremity exoskeletons and active orthoses: Challenges and state-of-the-art," *IEEE Trans. Robot.*, vol. 24, no. 1, pp. 144–158, Feb. 2008.
[14] S. H. Collins, M. B. Wiggin, and G. S. Sawicki, "Reducing the energy cost of human walking using an unpowered exoskeleton," *Nature*, vol. 522, no. 7555, pp. 212–215, 2015.
[15] L. Visser, R. Carloni, and S. Stramigioli, "Variable stiffness actuators: a port-based analysis and a comparison of energy efficiency," in *Proc. IEEE Int. Conf. Robot. Autom.*, 2010, pp. 3279–3284.
[16] B.-S. Kim and J.-B. Song, "Design and control of a variable stiffness actuator based on adjustable moment arm," *IEEE Trans. Robot.*, vol. 28, no. 5, pp. 1145–1151, Oct. 2012.
[17] A. Jafari, N. G. Tsagarakis, and D. G. Caldwell, "A novel intrinsically energy efficient actuator with adjustable stiffness (AWAS)," *IEEE/ASME Trans. Mechatronics*, vol. 18, no. 1, pp. 355–365, Feb. 2013.
[18] B. Vanderborght, R. van Ham, D. Lefeber, T. Sugar, and K. Hollander, "Comparison of mechanical design and energy consumption of adaptable, passive-compliant actuators," *Int. J. Robot. Res.*, vol. 28, no. 1, pp. 90–103, 2009.
[19] L. Visser, R. Carloni, and S. Stramigioli, "Energy-efficient variable stiffness actuators," *IEEE Trans. Robot.*, vol. 27, no. 5, pp. 865–875, Oct. 2011.

[20] R. Van Ham, B. Vanderborght, M. Van Damme, B. Verrelst, and D. Lefeber, "MACCEPA, the mechanically adjustable compliance and controllable equilibrium position actuator: Design and implementation in a biped robot," *Robot. Auton. Syst.*, vol. 55, no. 10, pp. 761–768, 2007.

[21] D. Braun, S. Apte, O. Adiyatov, A. Dahiya, and N. Hogan, "Compliant actuation for energy efficient impedance modulation," in *Proc. IEEE Int. Conf. Robot. Autom.*, 2016, pp. 636–641.

[22] N. Hogan, "Adaptive control of mechanical impedance by coactivation of antagonist muscles," *IEEE Trans. Automat. Control*, vol. 29, no. 8, pp. 681–690, Aug. 1984.

[23] C. E. English, "Implementation of variable joint stiffness through antagonistic actuation using rolamite springs," *Mech. Mach. Theory*, vol. 34, no. 1, pp. 27–40, 1999.

[24] S. Diller, C. Majidi, and S. H. Collins, "A lightweight, low-power electroadhesive clutch and spring for exoskeleton actuation," in *Proc. IEEE Int. Conf. Robot. Autom.*, 2016, pp. 682–689.